

AperTO - Archivio Istituzionale Open Access dell'Università di Torino

Interlayer tunneling spectroscopy of mixed-phase BSCCO superconducting whiskers

This is the author's manuscript

Original Citation:

Availability:

This version is available <http://hdl.handle.net/2318/1574031> since 2016-10-10T10:15:42Z

Published version:

DOI:10.1088/0953-2048/29/6/065013

Terms of use:

Open Access

Anyone can freely access the full text of works made available as "Open Access". Works made available under a Creative Commons license can be used according to the terms and conditions of said license. Use of all other works requires consent of the right holder (author or publisher) if not exempted from copyright protection by the applicable law.

(Article begins on next page)

This is the author's final version of the contribution published as:

O. Kizilaslan, Y. Simsek , M. A. Aksan , M. Truccato, Y. Koval and P. Müller

Interlayer Tunneling Spectroscopy of Mixed-Phase BSCCO Superconducting Whiskers

Superconductor Science Technology. 25 (10), 105003, (2012)

DOI: 10.1088/0953-2048/25/10/105003

The publisher's version is available at:

<http://iopscience.iop.org/article/10.1088/0953-2048/29/6/065013>

When citing, please refer to the published version.

Link to this full text:

<http://hdl.handle.net/>

This full text was downloaded from iris-Aperto: <https://iris.unito.it/>

Interlayer Tunneling Spectroscopy of Mixed-Phase BSCCO Superconducting Whiskers

O. Kizilaslan¹, Y. Simsek², M. A. Aksan³, M. Truccato⁴ Y. Koval² and P. Müller²

¹*Inonu University, Department of Biomedical Engineering, Faculty of Engineering
44280, Malatya, Turkey*

²*University of Erlangen, Department of Physics, 91058 Erlangen, Germany*

³*Inonu University, Faculty of Sciences and Arts, Department of Physics, 44280
Malatya, Turkey*

⁴*CNISM and NIS Center of Excellence, Department of Physics, University of Torino, Via P.
Giuria 1, I-10125, Torino, Italy*

ABSTRACT

In this work, we present a study on the interlayer tunneling spectroscopy of the mixed-phase BiSrCaCuO (BSCCO) superconducting whiskers. Cross-whisker junctions were prepared only by an annealing process without requiring a long lithography processes. The tunneling experiments were carried out on the cross-whisker junctions. A multiple superconducting energy gap in the cross-whisker junctions was observed, which is attributed to the presence of different doping levels of two $\text{Bi}_2\text{Sr}_2\text{CaCu}_2\text{O}_{8+\delta}$ phases (Bi-2212) rather than two different phases, $\text{Bi}_2\text{Sr}_2\text{CaCu}_2\text{O}_{8+\delta}$ and $\text{Bi}_2\text{Sr}_2\text{Ca}_2\text{Cu}_3\text{O}_{8+\delta}$ (Bi-2212 and Bi-2223) in the BSCCO whiskers. The temperature dependence of the energy gaps were discussed in framework of the BCS temperature-dependence. On the other hand, the carrier concentration of the cross-whisker junction was changed by carrier injection process. Effects of the carrier injection on the critical current, I_c , and the interlayer tunneling spectroscopy (ITS) of intrinsic Josephson junctions (IJJ's) were investigated in details.

High- T_c superconducting BiSrCaCuO (BSCCO) system has a layered crystal structure along the c -axis in which the superconducting CuO_2 layers alternate with BiO and SrO layers [1]. Weak interlayer coupling between the layers along c -axis leads to the formation of the atomic-scale intrinsic tunneling junctions. The interlayer tunneling spectroscopy (ITS) is an effective technique to determine both the superconducting energy gap and the quasi-particle density of state [2-4]. The tunneling spectroscopy provides a unique opportunity to probe bulk electronic properties of the crystal stack, independently from the adverse effect of sample surface.

Y. Koval et al. [5,6] reported that the superconductivity of the $\text{Bi}_2\text{Sr}_2\text{CaCu}_2\text{O}_{8+\delta}$ single crystals can be tuned by carrier injection process. Additionally, the carrier injection allows to study on the same sample without changing the chemical composition. When an intensive current is applied along the c -axis, the accelerated electrons are trapped eventually in the SrO or BiO layers. By a charge compensation, these electrons trapped in the insulator layers induce the change of the hole concentration in the superconducting planes. Simultaneously, the trapped electrons give rise to an intrinsic electrostatic field inside crystal and the field invokes the hole doping in the superconducting CuO_2 layer [7].

This study investigates the tunneling spectroscopy of the mixed-phase BSCCO single crystal whisker, $\text{Bi}_2\text{Sr}_2\text{CaCu}_2\text{O}_{8+\delta}$ and $\text{Bi}_2\text{Sr}_2\text{Ca}_2\text{Cu}_3\text{O}_{8+\delta}$ (Bi-2212 and Bi-2223). The tunneling spectroscopy experiments were carried out on the cross-whisker junction to investigate the superconducting energy gap, Δ_S , of the mixed-phase BSCCO whisker. Temperature dependence (T-dependence) of the energy gaps was also discussed. The evolution of the superconducting energy gap by carrier injection was investigated.

Three different cross-whisker junctions were prepared in this study. The first two junctions were used to characterize the cross-whisker junctions fabricated using the mixed-phase BSCCO whiskers. The other was used to investigate the evolution of the superconducting energy gap by the carrier injection. Whiskers in the present study were grown on the BSCCO glass plates prepared by the glass-ceramic technique. Detailed information on the whisker growth can be found in ref. [8]. It was found that the fabricated whiskers were in the underdoped region and possessed two different phases (Bi-2212 and Bi-2223) with $T_{c(0)}$ of ~ 68 K and 105 K, respectively.

In order to prepare the junctions, two different whiskers were mounted crosswise with an angle of 90 degrees on a MgO (100) substrate [9,10]. Cross-bars were post-annealed in air at 840°C for 30 min.

The obtained crystal stacks consisted of N (the number of intrinsic Josephson junctions, IJJ's) =12 (denoted as #WHS-CRS-3), 8 (denoted as #WHS-CRS-4) and 16 (denoted as #WHS-CRS-5) IJJ's. Figure 1(b) shows an enlarged view of the interface between the two whiskers. It can be seen from Figure 1(b) that we obtained a tunneling barrier at the interface, which is a result of interdiffusion during post-annealing, as well as intrinsic Josephson junctions.

Figure 2 shows the resistance vs. temperature curves of a cross-whisker junction #WHS-CRS-3, which has both artificial junction and intrinsic Josephson junctions. Three different phase transitions are observed. The first transition around 107 K corresponds to Bi-2223 while the second one around 82 K to Bi-2212. Normally, after the second transition, the resistance should go to zero, i.e. into the superconducting state. However, in our case there still exists a finite resistance around 73K. This resistance is due to the damaged interface layer (see figure 1(b)) produced during post-annealing. If the layer would be thin enough, Josephson coupling could set in, and resistance would go to zero at low enough temperatures in which the thermal energy $k_B T$ is sufficiently small. The critical temperature in which Josephson coupling starts is called T_J (indicated by an arrow in figure 2). Of course, zero resistance would mean that we have obtained a new artificial Josephson junction in addition to the adjacent intrinsic Josephson junctions.

In order to show whether or not the cross-whisker junctions fabricated using the mixed-phase BSCCO whiskers exhibits ideal junction characteristic, I-V characteristic of a cross-whisker junction was measured. T-dependence of I-V characteristic for a cross-whisker junction fabricated is shown in Figure 3. Inset of the figure 3 shows the T-dependence of normal state resistance, R_n , calculated from the slope of normal state portion of the tunneling I-V curves. Normal state resistance increased by ~1.56 % with increasing temperature from 4.2 K to 60.7 K. This is evidence that the junctions showed almost pure tunnel junction behavior because R_n in the tunnel junction is the temperature independent [11].

Δ_S can be determined from the sharp conductance peak at ITS characteristic. The gap, from zero voltage to the sharp peak, gives Δ_S ($V = 2\Delta/e$). Figure 4 shows the ITS characteristic of the cross-whisker per junction at different temperatures.

As emphasized above, the single-crystal whiskers used for the junctions showed two different phase transitions as Bi-2212 and Bi-2223. It is expected that electrical current flows between these phases in the superconducting state [12] and then two different conductance peaks at ITS characteristic due to tunneling.

One can claim that the first peak at low energy region corresponds to the energy gap ($\Delta_{Bi-2212}$) of the Bi-2212 phase, while the second peak at higher region to the energy gap ($\Delta_{Bi-2223}$) of the Bi-2223 phase. However, The detailed quantitative analysis of Δ_S of the crystal stacks are presented as a function of the temperature in figure 5 and the T-dependence of the peak at higher voltage (Δ_{higher}) indicates that Δ_{higher} collapsed almost at the same temperature as the peak at lower voltage (Δ_{lower}). Whereas the superconductivity for Bi-2223 is expected to disappear above 105 K. This is evidence that this difference is due to different doping levels of two Bi-2212 phases that have more or less the same T_c . About the heat treatment, that was necessary to join the whiskers, this is expected to produce an O-depleted region at the boundary between the (more or less square) junction area and the external environment. The thickness of the external O-depleted region depends on the duration of the heat treatment and it is expected that this region has lower doping level, if it is compared to other regions of whisker. Both of these regions are expected to contribute to both the c-axis R-T and I-V measurements as two in-parallel resistances.

Bi-2223 phase always appears as an intergrowth phase, which means that it is made up of filaments running along the a-axis, just one-cell thick in the c-axis direction [13]. Although they are detectable in the R vs T measurement when current is flowing along the a-axis because the cumulative length of all of the filaments is not negligible, the Bi-2223 volume is very small (much less than 0.5%) and a picture which depicts this situation can be found in Fig.8 of ref [14]. This might be another reason which supports the idea that two different conductance peaks at ITS characteristic are due to different doping level of two Bi-2212 phase rather than two different phases such as Bi-2212 and Bi-2223.

In figure 5b, a second data was also given to show the reproducibility of experimental results. Data were fitted to the BCS T-dependence [15] given by

$$\Delta(T) = \Delta(0) \tanh[A(B((T_c/T) - 1))^C]$$

Here, A, B and C are fitting parameters and were found to be 1.82, 1.018 and 0.51, respectively. T-dependence of both Δ_{lower} and Δ_{higher} shows a parabolic decrease with increasing temperature and a collapse of the gaps at temperatures close to T_c , figure 5a and b. However, a deviation from the BCS T-dependence was observed, indicating that the gaps dropped slightly more rapidly than the BCS prediction. The temperature dependence might be influenced by proximity effect between material of the different phases

(intergrowth Bi-2212/Bi-2223 system) and this can explain the deviation from BCS prediction.

If the two peaks in ITS characteristic correspond to superconducting gap of different doping levels of two Bi-2212 phases, as we suggested, it would be expected that the doping dependence of the peaks should also display similar characteristic. For this reason, it was investigated how the peaks change by carrier injection on one and the same sample. Carrier injection experiments were carried out on another cross-whisker junction (#WHS-CRS-5). For carrier injection doping at 4.2 K, a current in the range of 7.31 – 8.63 mA has been injected into the sample #WHS-CRS-5 along the *c*-axis, figure 6. It was found that at these current values, all of 16 IJJ's in this sample were in the resistive state. At such high bias, the voltage at constant current started to decrease. When the bias voltage drop reached a saturation value, the current was increased again and the procedure was repeated several times. After carrier injection process, the doping level of the crystal stack increased from 0.106 to 0.112 holes/Cu atom. The detailed information about the physical mechanism behind hole doping by the carrier injection is given in [5,7].

This effect is reversible [5]. In order to obtain the undoping effect, the bias current was increased in the range of 10.44 – 11.19 mA at 4.2 K and the voltage on the sample increased again in a constant current mode and the crystal stack shifted to highly underdoped state (holes number /Cu atom, $p=0.104$).

After both doping and undoping process by the carrier injection, I-V characteristics of the cross-whisker junction were measured at 4.2 K, figure 7. Initially, the junctions had very small critical current, I_c . Doping of the crystal stack by the carrier injection led to an increase by $\sim 24\%$ at I_c of the IJJ's. On the other hand, I_c of IJJ's decreased by $\sim 26\%$ after the undoping process. Additionally, it is seen that the voltage value, at which superconductivity disappeared, shifted to lower values. Inset of figure 7 shows one by one switching of the junctions into the resistive state, in which multiple quasi-particle structures appeared. It was found that I_c of the quasi-particle branches are significantly different from each other, indicating the presence of inhomogeneous state in the underdoped region.

Figure 8a shows ITS characteristics in different doping levels. After carrier doping by carrier injection, the peaks became sharper than ones after the undoping process. Zero-bias peak due to Josephson current increased by carrier injection, which indicates the change in the carrier concentration. Figure 8b presents the detailed analysis of the doping dependence of I_c and Δ_s . It is difficult to determine a unique I_c for the crystal stack in the underdoped region because of the highly inhomogeneous state. Therefore, the junction with the highest I_c was

analyzed. It can be clearly seen that the carrier injection effect caused an exponential increase at I_c , while Δ_s exponentially decreased with increasing the doping level. There are also several studies in the literature, which indicate that the c -axis critical current density, J_c , changes exponentially with the doping level or oxygen excess δ [16-18].

It was reported that there is a large inhomogeneity among the I_c values of quasiparticle branches in the underdoped region [5]. Similar results to ref [5] were observed for a minimum of 0.35 mA and a maximum of 3.5 mA in the cross-whisker junctions, inset of figure 7. Such a large inhomogeneous state leads to a highly incoherent interlayer tunneling within the crystal stack and thus to a significant decrease in Δ_s . Similarly, the anticorrelation between $I_c R_n$ and Δ_s in the underdoped Bi-2212 was previously reported [19,20].

In conclusion, we have showed that multiple superconducting energy gaps at ITS characteristic are due to different doping levels of two Bi-2212 phases rather than two different phases. Δ_s showed a parabolic decrease with temperature but a deviation from the BCS T -dependence was obtained. This was attributed to proximity effect. The results for three different samples showed that the cross-whisker junctions fabricated by the mixed-phase crystal stacks are reproducible. Additionally, the effect of the carrier injection on ITS characteristic of the mixed-phase BSCCO cross-whisker junction was investigated. An exponential increase in I_c was observed after carrier doping by carrier injection, while Δ_s exponentially decreased. The anticorrelation between I_c and Δ_s indicated the presence of incoherent c -axis transport in the underdoped BSCCO crystal stack.

Acknowledgement

This work was supported by Scientific and Technological Research Council of Turkey under contracts no TUBITAK-114F203.

References:

- [1] R. Kleiner, F. Steinmeyer, G. Kunkel, P. Müller, Intrinsic Josephson effects in $\text{Bi}_2\text{Sr}_2\text{CaCu}_2\text{O}_8$ single crystals, **Phys. Rev. Lett.** 68 (1992) 2394.
- [2] Minoru Suzuki, Takao Watanabe, and Azusa Matsuda, Interlayer tunneling spectroscopy for slightly overdoped $\text{Bi}_2\text{Sr}_2\text{CaCu}_2\text{O}_{8+\delta}$, **Phys. Rev. Lett.** 82 (1999) 5361.
- [3] K. Schlenga, R. Kleiner, G. Hechtfisher, M. Mößle, S. Schmitt, Paul Müller, Ch. Helm, Ch. Preis, F. Forsthofer, J. Keller H. L. Johnso, M. Veith and E. Steinbeiß, Tunneling spectroscopy with intrinsic Josephson junctions in $\text{Bi}_2\text{Sr}_2\text{CaCu}_2\text{O}_{8+\delta}$ and $\text{Tl}_2\text{Ba}_2\text{Ca}_2\text{Cu}_3\text{O}_{10+\delta}$, **Phys. Rev. B** 57 (1998) 14518.
- [4] Ø. Fischer, M. Kugler, I. Maggio-Aprile, and C. Berthod, Scanning tunneling spectroscopy of high-temperature superconductors, **Rev. Mod. Phys.** 79 (2007) 353.
- [5] Y. Koval, X. Jin, C. Bergman, Y. Simsek, L. Özyüzer, P. Müller, H. Wang, G. Behr, B. Büchner, Tuning superconductivity by carrier injection, **Appl. Phys. Lett.** 96 (2010) 082507.
- [6] Y. Koval, F. Chowdhury, X. Jin, Y. Simsek, F. Lichtenberg, R. Pentcheva,, P. Müller, Resistive memory switching in layered oxides: $\text{A}_n\text{B}_n\text{O}_{3n+2}$ perovskite derivatives and $\text{Bi}_2\text{Sr}_2\text{CaCu}_2\text{O}_{8+\delta}$ high- T_c superconductor, **Phys. Stat. Sol. A** 208 (2011) 284.
- [7] Y. Simsek, Y. Koval, K. Gieb and P. Müller, Superconductivity induced by carrier injection into non-superconducting $\text{Bi}_2\text{Sr}_2\text{CaCu}_2\text{O}_{8+\delta}$, **Supercond. Sci. Technol.** 27 (2014) 095011
- [8] O. Kizilaslan, M.A. Aksan, Crystallization of glass-ceramic $\text{Bi}_3\text{Sr}_2\text{Ca}_2\text{Cu}_3\text{O}_y$ superconducting system, **Journal of Crystal Growth** 381 (2013) 77.
- [9] Y. Takano, T. Hatano, A. Fukuyo, A. Ishii, M. Ohmori, S. Arisawa, K. Togano and M. Tachiki, d-like symmetry of the order parameter and intrinsic Josephson effects in $\text{Bi}_2\text{Sr}_2\text{CaCu}_2\text{O}_{8+\delta}$ cross-whisker junctions, **Phys. Rev. B** 65 (2002) 140513.
- [10] Y. I. Latyshev, A. P. Orlov, A. M. Nikitina, P. Monceau, R. A. Klemm, c-axis transport in naturally grown $\text{Bi}_2\text{Sr}_2\text{CaCu}_2\text{O}_{8+\delta}$ cross-whisker junctions, **Phys. Rev. B** 70 (2004) 094517.
- [11] V. M. Krasnov, A. Yurgens, D. Winkler, P. Delsing, and T. Claeson, Evidence for Coexistence of the Superconducting Gap and the Pseudogap in Bi-2212 from Intrinsic Tunneling Spectroscopy, **Phys. Rev. Lett.** 84 (2000) 25.

- [12] I. Giaever, Electron tunneling between two superconductors, **Phys. Rev. Lett.** 5 (1960) 464.
- [13] Y. Zhao, G. D. Gu, G. J. Russel, N. Nakamura, S. Tajima, J. G. Wen, K. Uehara and N. Koshizuka, Normal-state reentrant behavior in superconducting $\text{Bi}_2\text{Sr}_2\text{CaCu}_2\text{O}_8$ and $\text{Bi}_2\text{Sr}_2\text{CaCu}_2\text{O}_{10}$ intergrowth single crystals, **Phys. Rev. B** 51 (1995) 3134–9.
- [14] M. Truccato, D. Imbraguglio, A. Agostino, S. Cagliero, A. Pagliero, H. Motzkau and A. Rydh, Photoconductivity effects in mixed-phase BSCCO whiskers, **Supercond. Sci. Technol.** 25 (2012) 105010 (13pp).
- [15] A. Carrington, F. Manzano, Magnetic penetration depth of MgB_2 , **Physica C** 385 (2003) 205–214.
- [16] M. Suzuki, T. Hamatani, Y. Yamada, K. Anagawa, T. Watanabe, Maximum Josephson current and inhomogeneous superconductivity in $\text{Bi}_2\text{Sr}_2\text{CaCu}_2\text{O}_{8+\delta}$, **J. of Physics: Conference Series** 43 (2006) 1110.
- [17] H. Kambara, I. Kakeya, M. Suzuki, Intrinsic Tunneling Spectroscopy for Pb-Substituted Bi_{2212} in the Underdoped Region, **J. of Physics: Conference Series** 400 (2012) 022043.
- [18] S. Probst, X.Y. Jin, Y. Simsek, C. Steiner, C. Bergmann, Y. Koval, P. Müller, *Intrinsic Josephson effects in $\text{Bi}_2\text{Sr}_2\text{CaCu}_2\text{O}_{8+\delta}$ after doping by current injection*, Bull. Am. Phys. Soc (2011) V2300008.
- [19] V. M. Krasnov, Interlayer tunneling spectroscopy of $\text{Bi}_2\text{Sr}_2\text{CaCu}_2\text{O}_{8+\delta}$: A look from inside on the doping phase diagram of high- T_c superconductors, **Phys. Rev. B**, 65 (2002) 140504.
- [20] H. Motzkau, T. Jacobs, S.O Katterwe, A. Rydh, and V. M. Krasnov, Persistent electrical doping of $\text{Bi}_2\text{Sr}_2\text{CaCu}_2\text{O}_{8+x}$ mesa structures, **Phys. Rev. B**, 85 (2012) 144519.

Figure Captions

Figure 1. (a) Sketch of the sample design, (b) enlarged view of the interface between two whiskers. The black layers mark the CuO planes, and the light blocks mark the insulating layer, the red layer in between is the interface layer.

Figure 2 . Resistance vs. temperature characteristics of cross-whisker junction, #WHS-CRS-3.

Figure 3. T-dependence of I-V characteristic of the cross-whisker junction, #WHS-CRS-3. Inset shows the T-dependence of normal state resistance, R_n .

Figure 4. The ITS characteristics of cross-whisker junctions fabricated by mixed-phase BSCCO (Bi-2212/Bi-2223) at different temperatures, #WHS-CRS-3 sample. The figure on the right side was given for clarity.

Figure 5. Δ_S values at different temperatures: a) #WHS-CRS-3 sample, b) #WHS-CRS-4 sample. The half-filled symbols and the full-filled symbols show the T-dependence of Δ_{2212} and the T-dependence of Δ_{2223} , respectively. Solid lines show the BCS T-dependence for Bi-2212 and Bi-2223 phases.

Figure 6. Carrier injection procedure performed manually on the sample #WHS-CRS-5. Inset shows an enlarged view of the voltage drop.

Figure 7. I-V characteristics of the sample #WHS-CRS-5 after both the doping and undoping process. Inset shows all of 16 quasiparticle branches.

Figure 8. a) The evolution of ITS characteristic of the cross-whisker junction after both doping and undoping by carrier injection, b) the detailed analysis of the doping dependence of I_c and Δ_s at lower voltage.

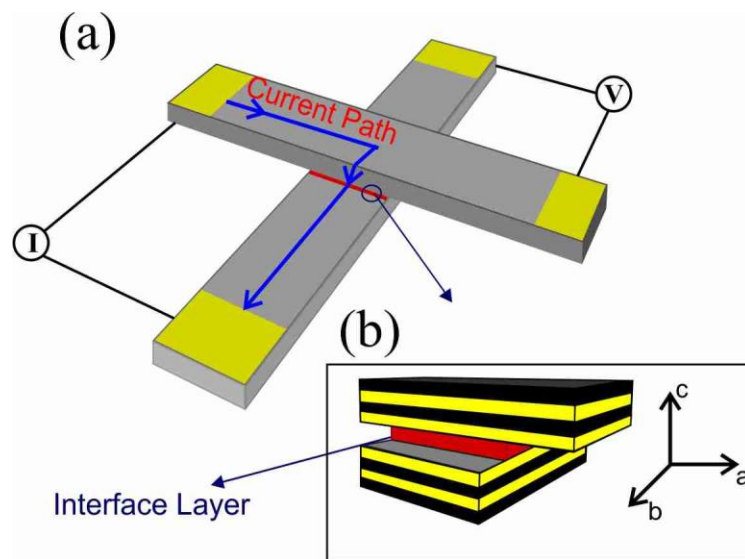


Figure 1.

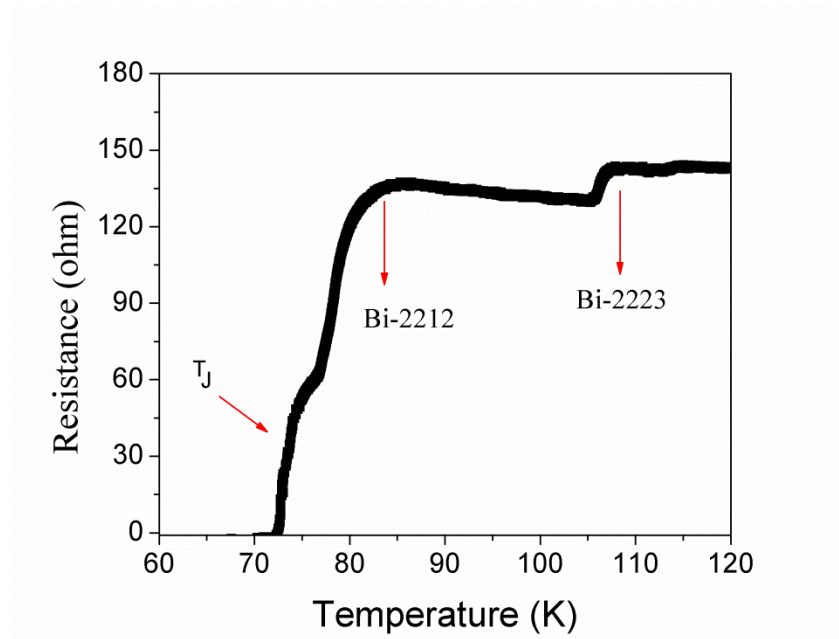


Figure 2.

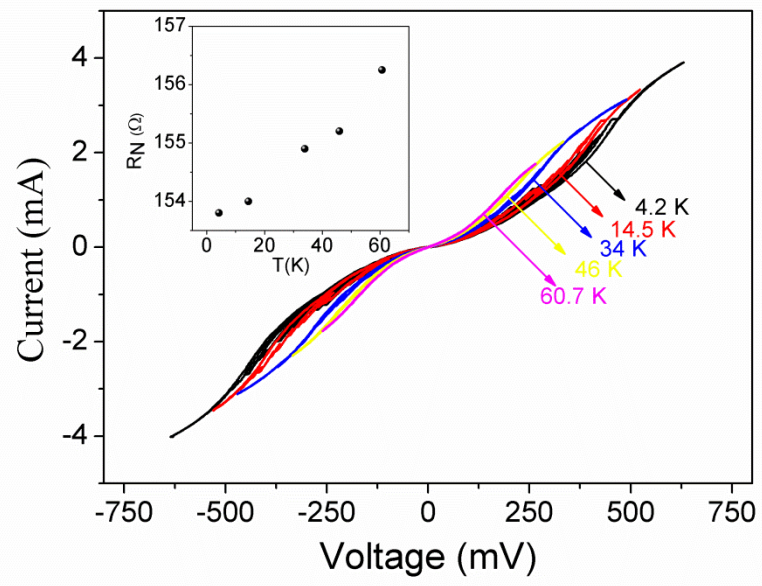


Figure 3.

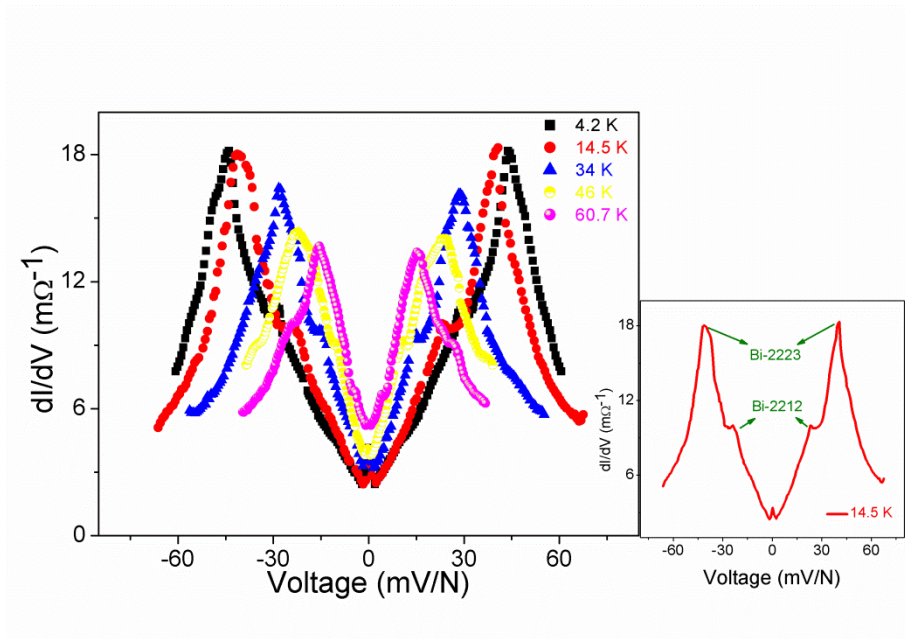


Figure 4.

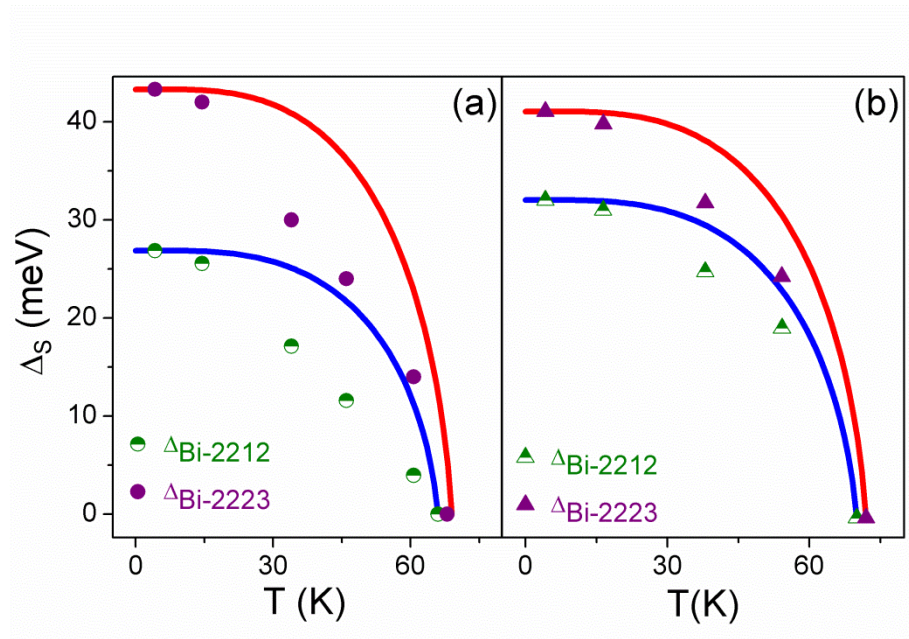


Figure 5.

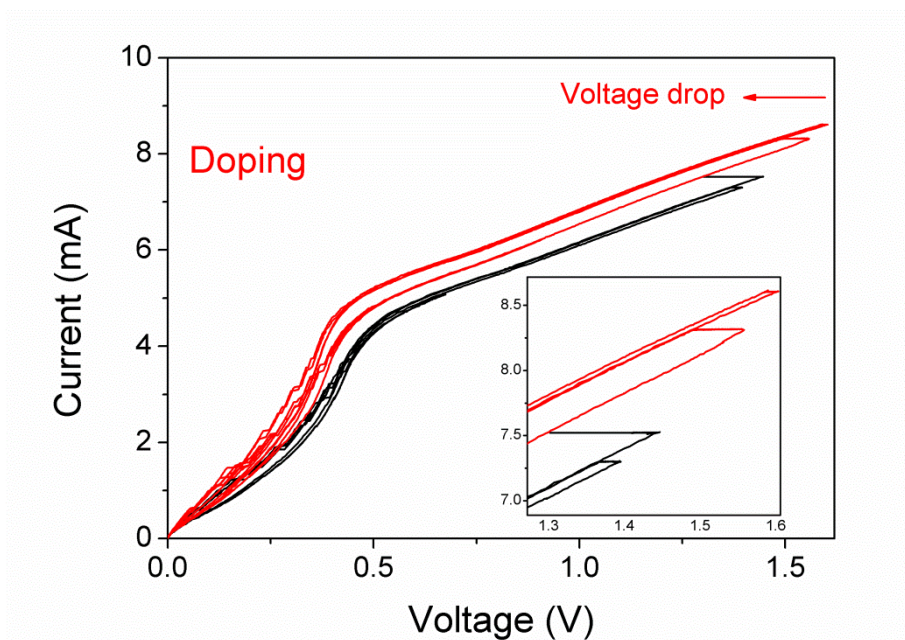


Figure 6.

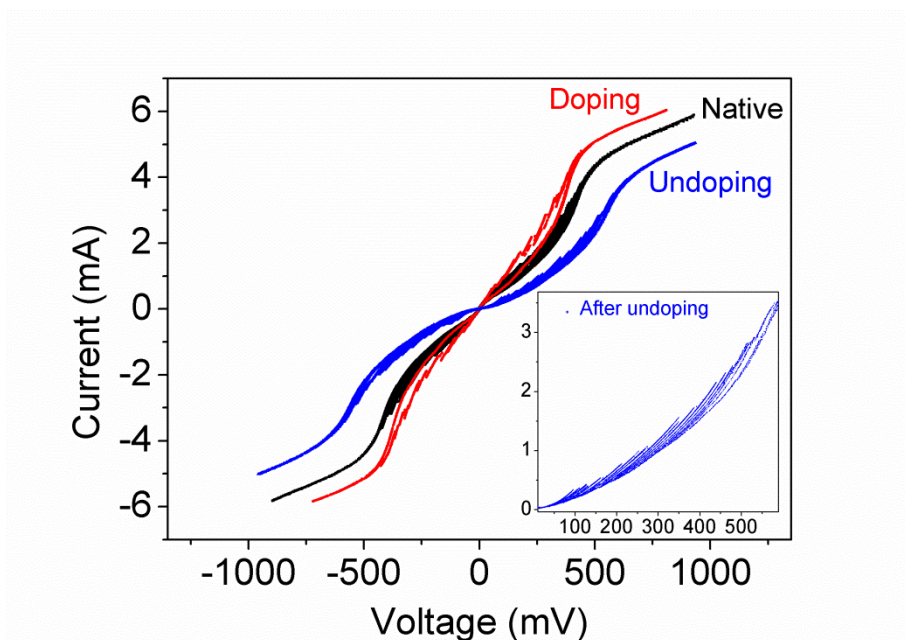


Figure 7.

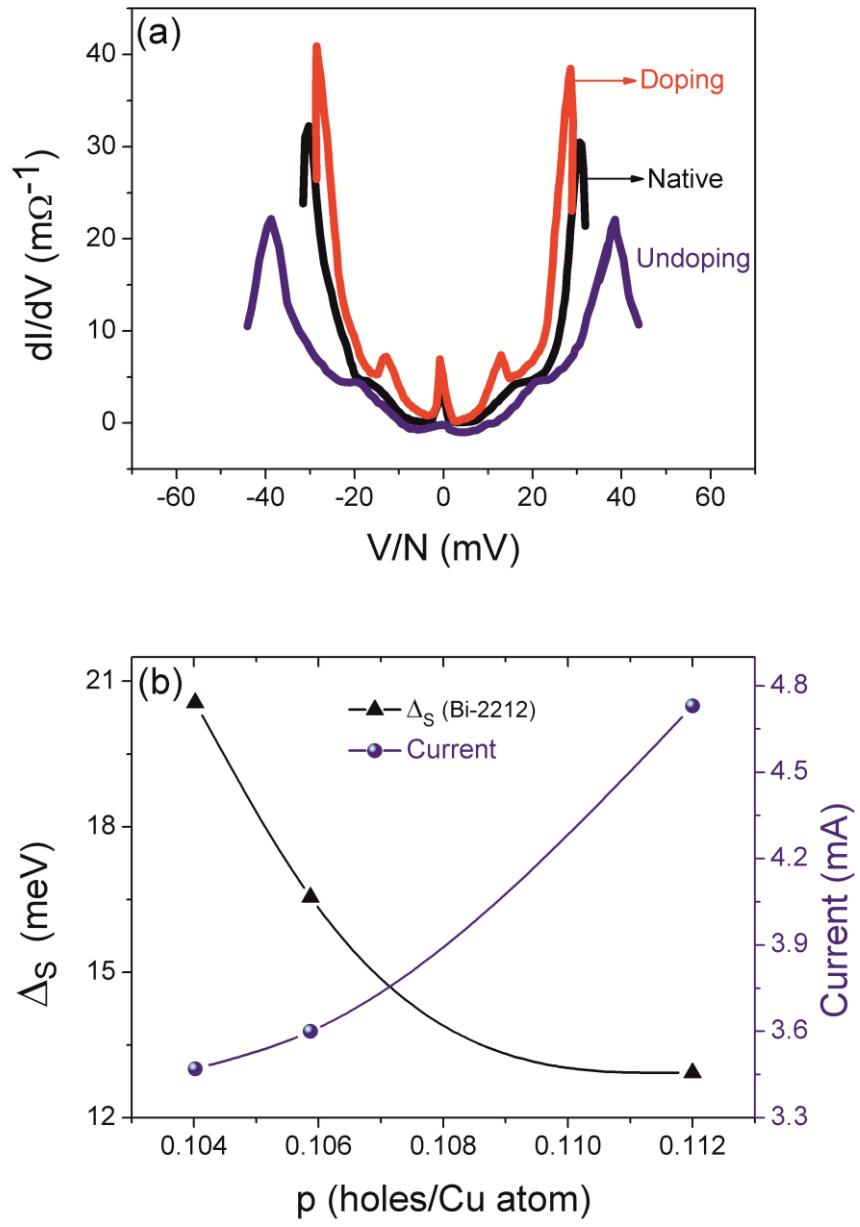


Figure 8.